THE JOURNAL OF BIOLOGICAL CHEMISTRY
Vol. 277, No. 46, Issue of November 15, pp. 44050–44060, 2002

Printed in U.S.A.

SDS-resistant Active and Thermostable Dimers Are Obtained from the Dissociation of Homotetrameric β-Glycosidase from Hyperthermophilic *Sulfolobus solfataricus* in SDS

STABILIZING ROLE OF THE A-C INTERMONOMERIC INTERFACE*

Received for publication, July 8, 2002, and in revised form, September 3, 2002
Published, JBC Papers in Press, September 3, 2002, DOI 10.1074/jbc.M206761200

Fabrizio Gentile‡, Pietro Amodeo§, Ferdinando Febbraio¶‖, Francesco Picaro‡, Andrea Motta§, Silvestro Formisano‡, and Roberto Nucci¶

From the ‡Istituto di Endocrinologia e Oncologia Sperimentale del CNR and Dipartimento di Biologia e Patologia Cellulare e Molecolare, Università Federico II, Via Pansini 5, 80131 Napoli, §Istituto di Chimica Biomolecolare del CNR, Via Campi Flegrei 34, 80078 Pozzvoli, Napoli, and ¶Istituto di Biochimica delle Proteine del CNR, Via Marconi 10, 80125 Napoli, Italy

β-Glycosidases are fundamental, widely conserved enzymes. Those from hyperthermophiles exhibit unusual stabilities toward various perturbants. Previous work with homotetrameric β-glycosidase from hyperthermophilic *Sulfolobus solfataricus* (M_r 226,760) has shown that addition of 0.05–0.1% SDS was associated with minimal secondary structure perturbations and increased activity. This work addresses the effects of SDS on β-glycosidase quaternary structure. In 0.1–1% SDS, the enzyme was dimeric, as determined by Ferguson analysis of transverse-gradient polyacrylamide gels. The catalytic activity of the β-glycosidase dimer in SDS was determined by in-gel assay. A minor decrease of thermal stability in SDS was observed after exposure to temperatures up to 80 °C for 1 h. An analysis of β-glycosidase crystal structure showed different changes in solvent-accessible surface area on going from the tetramer to the two possible dimers (A-C and A-D). Energy minimization and molecular dynamics calculations showed that the A-C dimer, exhibiting the lowest exposed surface area, was more stabilized by a network of polar interactions. The charge distribution around the A-C interface was characterized by a local short range anisotropy, resulting in an unfavorable interaction with SDS. This paper provides a detailed description of an SDS-resistant inter-monomeric interface, which may help understand similar interfaces involved in important biological processes.

Enzymes from hyperthermophiles are interesting for the possible biotechnological applications of their unusual stability toward a number of perturbing agents, including extremes of temperature, pH, ionic strength, and detergents. In particular, the structural determinants of protein resistance to denaturation and dissociation by SDS have recently become the focus of increasing attention, as SDS-resistant intermolecular interactions have been identified within the context of important biological functions. A correlation was found between the SDS stability of different heterodimeric products of the major histocompatibility complex class II polymorphic genes of the HLA complex and susceptibility to important human autoimmune diseases, such as insulin-dependent diabetes mellitus (IDDM)[1] (1). Moreover, the isoform-specific formation of SDS-stable complexes was observed between amyloid-β (Aβ), a major component of extracellular senile plaques of Alzheimer's disease (AD), and the apolipoproteins apoE2 and apoE3 but not with apoE4, which is present with increased frequency in patients with sporadic and late-onset familial AD, and is considered a risk factor for the disease (2, 3). Investigations of the mechanistic basis of these SDS-stable interactions have pinpointed some of the critical amino acid residues and the interactions involved (4–7).

Proteins from hyperthermophilic organisms are ideally suited for the study of the structural determinants of protein stability, in view of their physicochemical resistance, higher phylogenetic proximity to eukaryotic enzymes, in comparison with prokaryotic counterparts, and high yields in recombinant expression systems. Among these, β-glycosidase from the hyperthermophilic Archaea *Sulfolobus solfataricus* (Sβgly) strain MT4 (8) is one of the best characterized. It is a member of a large superfamily of enzymes, widely conserved among animals, plants, Archaea, and bacteria, some of which are responsible for the pathogenesis of important human diseases (9). Sβgly is a homotetramer of four, non-covalently linked, identical subunits, each having a relative molecular mass of 56,690. It is highly thermostable, having a $t_{½}$ of 85 h at 75 °C. The native enzyme has been crystallized, and its structure has been resolved at 2.6 Å (10), consisting of a $(\beta/\alpha)_8$ barrel, typical of enzymes of glycosylhydrolase family 1 (11).

We have shown previously that the exposure of Sβgly to SDS in the concentration range of 0.05–0.1% resulted in an increase of its enzymatic activity at room temperature (12). CD spectra in the far-UV region and infrared spectroscopy at pH 10.0 showed negligible effects of SDS on the secondary structure of the enzyme, whereas more significant changes were observed in the protein tertiary structure by near-UV CD analysis (13).

The aim of the present study was to investigate the conse-

* The costs of publication of this article were defrayed in part by the payment of page charges. This article must therefore be hereby marked "*advertisement*" in accordance with 18 U.S.C. Section 1734 solely to indicate this fact.

‖ To whom correspondence should be addressed: Ferdinando Febbraio Istituto di Biochimica delle Proteine del CNR, Via Marconi 10, 80125 Napoli, Italy. Tel./Fax: +39-0817257300; E-mail: febbraio@dafne.ibpe.na.cnr.it.

[1] The abbreviations used are: IDDM, insulin-dependent diabetes mellitus; Aβ, amyloid-β; AD, Alzheimer's disease; apoE, apolipoprotein E; EM, energy minimization; MD, molecular dynamics; PDB, Protein Data Bank; PNPG, *p*-nitrophenyl-β-D-glucopyranoside; SAS, solvent-accessible surface; Sβgly, *S. solfataricus* β-glycosidase; T, total acrylamide; C, *N,N′*-methylene-bis-acrylamide, as percent of total acrylamide; X-gal, 5-bromo-4-chloro-3-indolyl-β-D-galactopyranoside.

quences of the interaction of Sβgly with SDS at the level of its quaternary structure, activity, and thermostability. Ferguson analysis of polyacrylamide gels in SDS clearly documented that the enzyme in SDS dissociated into dimers, which were shown to be fully active and to retain most of the thermal stability of the native tetrameric enzyme. Calculations of the solvent-accessible surfaces, as well as energy minimization (EM) calculations and molecular dynamics (MD) simulations of the possible oligomerization states of Sβgly, based on the crystal structure of the tetrameric enzyme (10), indicated that the interface between A-C (and B-D) monomers was stabilized by a network of polar interactions, characterized by an unfavorable interaction with SDS. On the basis of these observations, Sβgly can be envisioned as a dimer of SDS-resistant dimers.

The detailed description presented of such an SDS-resistant inter-monomeric interface may be useful, on a comparative basis, for our understanding of similar inter-subunit and protein-protein interfaces involved in important biological processes and for protein engineering purposes.

EXPERIMENTAL PROCEDURES

Purification and Protein Assay—Homogeneous Sβgly was prepared as described previously (8). The protein concentration was estimated by the optical absorbance at 280 nm, using a molar extinction coefficient of 9.5×10^5 cm^{-1} (8).

Enzyme Assay—The enzymatic activity was measured using 4 mM *p*-nitrophenyl-β-D-glucopyranoside (PNPG) as the substrate in a 1-ml final volume of 50 mM sodium phosphate buffer, pH 6.5, by monitoring the increase in absorbance at 405 nm. All the enzymatic assays were carried out in a thermostated Cary 1 spectrophotometer (Varian, Australia) at the temperature of 75 °C (8).

Sβgly Kinetic Constants and Thermostability in the Presence and Absence of SDS—The kinetic constants of Sβgly were measured in the temperature range from 30 to 80 °C (by stepwise increases of 10 °C), using PNPG concentrations in the range 0.1–20 mM in 1-ml reaction mixtures containing 50 mM sodium phosphate buffer, pH 6.5, in the presence or absence of 0.1% SDS. The experimental data were analyzed by using the data analysis and graphics program "Grafit" (Erithacus Software Ltd.).

Thermal stability of Sβgly was measured incubating 0.41 μM of the homogeneous enzyme in 0.1 M sodium phosphate buffer, pH 6.5, at temperatures ranging from 30 to 80 °C (by stepwise increases of 10 °C) in a thermostated water bath, in the presence and absence of 0.1% SDS. At time intervals, aliquots containing 4.1 pmol of enzyme were withdrawn from the incubation mixture and assayed at 75 °C under the conditions described.

Analytical SDS-PAGE of Sβgly—SDS-PAGE was performed using the discontinuous buffer system of Laemmli (14), in a Hoefer SE 600 vertical slab gel apparatus. A linear vertical gradient gel, containing 4–10% total acrylamide (T), 2.7% *N,N′*-methylenebisacrylamide (C, expressed as percent of total acrylamide), in 0.375 M Tris/HCl, pH 8.8, 0.1% SDS, was polymerized on a sheet of Gelbond PAG plastic backing (Bio-Whittaker). The acrylamide stock contained 29.8% (w/v) acrylamide, 0.2% (w/v) *N,N′*-methylenebisacrylamide, and 1% (v/v) AcrylAide (Bio-Whittaker) to allow covalent bonding to the Gelbond PAG. Stacking gels contained 3.75% T, 0.125 M Tris/HCl, pH 6.8, 0.1% SDS. Sβgly was dissolved in 0.01 M Tris/HCl, pH 6.8, 1% SDS, 0.7 M β-mercaptoethanol, 1.36 M glycerol, 0.005% bromphenol blue as tracking dye, with or without heating in a boiling water bath for 1 min. The electrode buffer contained 0.025 M Tris base, 0.19 M glycine, pH 8.2. Electrophoresis was conducted at 15 °C at 10 mA for 16 h. The following High Molecular Weight Standards for SDS-PAGE (Bio-Rad) were used as calibration proteins (relative molecular masses in parentheses): skeletal muscle myosin heavy chain (205,000), *Escherichia coli* β-galactosidase (116,000), phosphorylase *b* (94,000), bovine serum albumin (67,000), ovalbumin (45,000), and carbonic anhydrase (30,000). The gels were stained with 0.1% Coomassie Brilliant Blue R-250 in 25% (v/v) 2-propanol, 10% (v/v) acetic acid, destained in 25% (v/v) methanol, 10% acetic acid, equilibrated in 0.7 M glycerol, and air-dried.

Preparation of Linear Transverse-Gradient Polyacrylamide Gels—Linear transverse-gradient polyacrylamide gels were prepared as described (15), using a Hoefer SE 600 vertical slab gel apparatus. A linear vertical gradient was cast between two 160 × 180-mm glass plates positioned on one of their short sides as the base. After polymerization, the gel was turned 90° counterclockwise, so that the gradient was now perpendicular to the direction of electrophoresis (Fig. 2, *panel A*). The glass plates were held apart by three 1.5-mm-thick spacers as follows: a 20-mm-wide spacer along the base, to be left in place when turning the gel; a 20-mm-wide spacer on the right, to be removed when turning the gel in order to form a sample trough on the top of the gel and to be inserted at what was to become the left side of the gel; and a 10 mm-wide spacer on the left, to be removed upon turning the gel in order to leave an empty trough below the gel. The gels were polymerized on a sheet of Gelbond PAG adhering to one of the glass plates. The acrylamide stock contained 29.2% (w/v) acrylamide, 0.8% (w/v) *N,N′*-methylenebisacrylamide as cross-linker, without AcrylAide. Linear transverse-gradient gels containing 4–9% T from left to right, 2.7% C, in 0.375 M Tris/HCl, pH 8.8, 0.1% SDS, were made from two solutions with compositions of the ends of the desired gradient, with the aid of a two-chamber gradient mixer. No stacking gel was used, but a sample gel containing 3.75% T in electrode buffer was created by positioning a plastic comb in the sample trough on top of the gel, 1 mm apart from the upper side of the gel. For electrophoresis in SDS, reference standards and Sβgly were subjected to electrophoresis altogether in alternate lanes of a couple of identical 20-lane gels. The electrode buffer contained 0.025 M Tris base, 0.19 M glycine, pH 8.2. Sβgly was dissolved in 0.01 M Tris/HCl, pH 6.8, 1% SDS, 0.7 M β-mercaptoethanol, 1.36 M glycerol, 0.005% bromphenol blue as tracking dye, without boiling. Native linear transverse-gradient polyacrylamide gels containing 4–7% T, 2.7% C, in 0.187 M Tris/H_2SO_4, pH 9.0, were prepared in a similar manner, according to Neville (16). For electrophoresis in native conditions, reference standards and Sβgly were subjected individually to electrophoresis on a couple of identical 15-lane gels. The electrode buffer contained 0.065 M Tris base, 0.031 M boric acid, pH 9.3. Sβgly was dissolved in electrode buffer containing 1.36 M glycerol, 0.005% bromphenol blue. Both SDS and native electrophoresis were conducted at 15 °C at 10 mA, until the dye front reached the lower end on the left side of the gels. The gels were stained as described for analytical gels in SDS, equilibrated in 0.7 M glycerol, and dried under vacuum.

Relative Molecular Mass Estimation by Ferguson Analysis of Linear Transverse-Gradient Polyacrylamide Gels—The relative molecular mass (M) of Sβgly was determined by indirect comparison of the relative mobilities (R_m) of Sβgly and those of calibration proteins, after electrophoresis in a linear transverse-gradient polyacrylamide gel. To determine the R_m of a protein, its migration distance from the top of the separating gel to the center of the protein band (R_p) was divided by the migration distance of the bromphenol blue tracking dye (R_d). The %T along the linear transverse-gradient polyacrylamide gel was calculated by Equation 1,

$$\%T = (9.0 \text{ (or } 7.0) - 4.0) \times D/W + 4.0 \qquad \text{(Eq. 1)}$$

where W is the distance between the 4.0% T edge and the other edge (9.0% or 7.0%) of the gel, and D is the distance between the 4.0% T edge of the gel and the center of the protein zone. All distances were measured directly on the gels layered onto a square millimeter division; distances were read to the nearest 0.5 mm. From the R_m values determined for each protein at different polyacrylamide concentrations, a Ferguson plot ($100 \times \log(R_m \times 100)$ *versus* %T) was constructed (10 points per gel, 20 points per plot for gels in SDS; 15 points per gel, 30 points per plot for native gels), and the slope (retardation coefficient, K_r) was calculated by least square regression analysis, using %T as the argument. For the calibration proteins, the relationship between relative molecular mass and K_r, namely log M and log K_r, was calculated by least square regression analysis, using log M as the argument. On the basis of this relationship and the measured K_r of Sβgly, the relative molecular mass of Sβgly was determined. The reference proteins used for the construction of Ferguson plots in the presence of SDS were the High Molecular Weight Standards for SDS-PAGE supplied by Bio-Rad, already described for analytical SDS-PAGE. The calibration proteins used for the construction of Ferguson plots in the absence of SDS were as follows (relative molecular masses in parentheses): bovine thyroglobulin (660,000); horse spleen apoferritin (481,000) (17); sweet potato β-amylase (224,000); and alkaline phosphatase (140,000).

In-gel Assay of the Enzymatic Activity of Sβgly with X-Gal—Two 80 × 60 × 1.5-mm minigels containing 5% T in 0.375 M Tris/HCl, pH 8.6, with or without 0.1% SDS, were prepared without plastic backing, using the mini-Protean apparatus (Bio-Rad). The electrode and sample buffers used for electrophoresis in SDS were the same described for SDS-PAGE in linear transverse-gradient polyacrylamide gels. As for native PAGE, the electrode buffer containing 0.005 M Tris base, 0.038 M glycine, pH 8.2, and Sβgly was dissolved in electrode buffer with 10% glycerol, 0.005% bromphenol blue. At the end of electrophoresis, the gels were

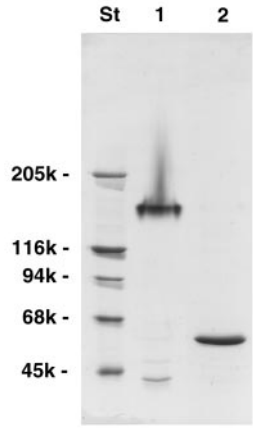

FIG. 1. **SDS-PAGE of *S. solfataricus* β-glycosidase.** Electrophoresis was conducted in Tris/glycine in 0.1% SDS, according to Laemmli (14), in a 4–10% T linear vertical gradient polyacrylamide gel. The gel was stained with Coomassie Brilliant Blue R-250. Relative molecular mass standards (*St*) are indicated. *Lane 1*, Sβgly prepared in SDS-PAGE loading buffer without boiling; *lane 2*, Sβgly subjected, prior to electrophoresis, to precipitation in methanol/chloroform/water (26).

equilibrated in two changes of 0.05 M sodium phosphate, pH 6.5, with or without 0.1% SDS, for 15 min each, and then incubated in 10% X-gal in 0.05 M sodium phosphate, pH 6.5, 10% (v/v) methanol, with or without 0.1% SDS, at 37 °C for 16 h.

Structure Calculations—Structures were refined by MD and EM calculations using the AMBER 4.1 package (18–20), with the AMBER94 All-Atom parametrization (21). Preliminary MD and EM calculations were performed *in vacuo*, with a distance-dependent dielectric constant $\epsilon = r$, to roughly reproduce solvation effects. In addition, a reduction from 1 to 0.2 of the absolute value of the total charge was used for acid and basic residues and for terminal NH^{3+} and COO^{-} groups, to avoid overstabilization of H-bonds and salt bridges. For the same reason, very short preliminary EM (less than 1000 steps) and MD calculations (less than 50 ps) were performed to remove sterical strain only, switching to MD runs with explicit solvation as soon as stable structures were obtained. This whole procedure should prevent from obtaining artificially compact structures, with overwhelming patterns of polar interactions acting as driving forces for both intra- and intermolecular interactions. Final refinement steps were run in a periodic water box. An 8-Å cut-off for non-bonded interactions was used in all the calculations. MD runs were performed with a time step of 2 fs (1.5 fs for MD at 368 K), using the SHAKE procedure (22) to constrain bond lengths, at temperatures of 300, 310, and 368 K and, in the case of simulations in water, a pressure of 1 atm. A coupling with an external bath of both heat and pressure (23) was applied, with time constants of 0.2 and 0.5 ps, respectively. The protocol used for starting model refinement included a preliminary EM *in vacuo*, followed by a 50-ps MD and a final EM to remove initial sterical strain. A 400-ps MD in a water box was then performed, and the structures corresponding to the last 200 ps of each trajectory were averaged for further analysis. The MD trajectories in water were sampled every 5 ps. The average and the final structure of the refinement procedure for each model were energy-minimized to obtain meaningful geometrical parameters in the structural validation and to perform those analyses for which either an average structure or a bundle of MD frames did not give a suitable representation of the system. The resulting structures were analyzed with the MOLMOL program (24), which was also used to produce all the molecular plots. The NACCESS program was used for the calculation of solvent accessibilities and buried areas; in this analysis, the standard values of the atomic van der Waals radii included in the program were used, with a spherical probe radius of 1.4 Å. The Cartesian coordinates of the hydrogen atoms, missing in the reference crystallographic structure, were calculated with the HBPLUS program (25), also used to perform further H-bond analysis.

RESULTS

Apparent Relative Molecular Mass of Sβgly in SDS-PAGE—The migration of Sβgly in a 4–10% total acrylamide (T) linear vertical gradient polyacrylamide gel is shown in Fig. 1. Sβgly migrated with an apparent relative molecular mass of about 160,000. On the other hand, Sβgly subjected to precipitation by the use of a 4:1:4 mixture of methanol/chloroform/water (26) migrated with an apparent relative molecular mass of 57,000, in agreement with the mass spectrometric measurement of 56,690 of the Sβgly monomer. Thus, it appears that the species with the apparent relative molecular mass of 160,000 represented an oligomeric form of Sβgly, with persisting quaternary structure under the conditions used for SDS-PAGE (exposure to 1% SDS in the sample buffer and 0.1% SDS in the gel and electrode buffers), whereas exposure to a mixture of organic solvents resulted in the complete dissociation of Sβgly into monomers. Because a trimer, with a calculated M_r of 170,070, was not predictable on the basis of the crystallographic symmetry (10), such an oligomeric form may either be an anomalously fast migrating tetramer or an anomalously slow migrating dimer.

Determination of the Relative Molecular Mass of Sβgly by Ferguson Plot-based Analysis of Polyacrylamide Gels in SDS—Ferguson plots of the logarithm of the relative mobility (R_m) of a protein at several different acrylamide concentrations against the gel concentration (T) provide an optimal means of determining the relative molecular mass of proteins exhibiting anomalous free mobility and R_m. If the concentration of the cross-linker, *i.e. N,N′*-methylenebisacrylamide, expressed as percentage of total acrylamide (C), is held constant, the values of the retardation coefficients (K_r), calculated from the linear relationship between log R_m and T for different proteins, are linearly related to their relative molecular masses (16, 27).

For the determination of the relative molecular mass of Sβgly during electrophoresis in the presence of SDS, a Ferguson plot was constructed, using 100 log 100 R_m *versus* log M, for a set of reference proteins, ranging in relative molecular mass from 45,000 to 205,000, and for Sβgly itself, after electrophoresis in Tris/glycine according to Laemmli (14), in the presence of 0.1% SDS, on two 4–9% T, 2.7% C transverse-gradient gels (4–10 points per gel, 8–20 points per plot). One such gel, in which the reference proteins and Sβgly occupy alternating lanes, is shown in Fig. 2, *panel A*, whereas the Ferguson plot is shown in Fig. 2, *panel B*. The values of K_r found are reported in Table I. The K_r values of the reference proteins were plotted against their respective values of M (Fig. 2, *panel C*), and the M of Sβgly was then interpolated from the mean square regression linking them. The Ferguson analysis indicated a relative molecular mass of 109,400 for Sβgly in the presence of 0.1% SDS, a value compatible with incomplete dissociation of Sβgly into dimers. All reference proteins, except the myosin heavy chain, had coinciding values of the apparent relative free mobility (Y_0) (*i.e.* the apparent relative mobility extrapolated to 0 acrylamide concentration), as it was expected on the base of previous descriptions of the behavior of a number of protein-SDS complexes (16). Instead, Sβgly and the myosin heavy chain exhibited a lower value of Y_0, a circumstance also suggesting anomalous electrophoretic migration (16).

Determination of the Relative Molecular Mass of Sβgly by Ferguson Plot-based Analysis of Native Polyacrylamide Gels—For the determination of the relative molecular mass of Sβgly during electrophoresis under native conditions, *i.e.* in the absence of SDS, a Ferguson plot was constructed, using 100 log 100 R_m *versus* log M, for a set of reference proteins, ranging in relative molecular mass from 140,000 to 660,000, and for Sβgly itself, after electrophoresis in Tris/boric acid, in the absence of SDS, according to Neville (16), on two 4–7% T, 2.7% C transverse-gradient gels per each standard and Sβgly (15 points per gel, 30 points per plot). The Ferguson plot is shown in Fig. 3, *panel A*. The values of K_r found are reported in Table I. The K_r values of the reference proteins were plotted against their

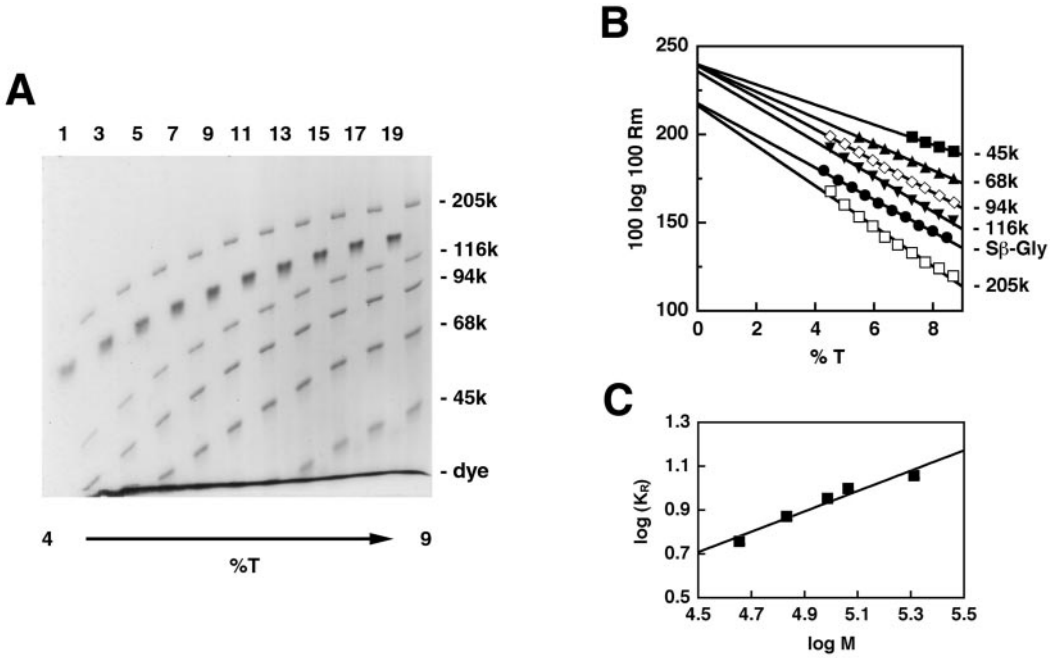

FIG. 2. **Ferguson analysis of the PAGE in SDS of *S. solfataricus* β-glycosidase.** *Panel A* shows one of two replicate 4–9% T, 2.7% C polyacrylamide transverse-gradient gels used for the determination of the relative molecular mass of Sβgly in 0.1% SDS by Ferguson analysis (29). Acrylamide concentration increased from the left to the right side of the gel. Electrophoresis was performed in Tris/glycine in 0.1% SDS (14). *Odd lanes* (*numbered* at the *top*) contained 2.5 μg each of Sβgly, and *even-numbered lanes* contained relative molecular mass standards (2 μg each), marked at the *right side* of the gel. The dye front is indicated. *Panel B* shows the Ferguson plot constructed for the set of reference proteins and Sβgly. For the sake of clarity, only one set of points from one of the two gels is shown. The values of K_r obtained are reported in Table I. In *panel C*, the plot of the log of measured K_r *versus* log M of the reference proteins used to interpolate the log M of Sβgly is shown.

TABLE I
Retardation coefficients (K_r) of molecular mass marker proteins and S. solfataricus β-glycosidase in SDS-PAGE and native PAGE

Protein	M	K_r	r^a
SDS-PAGE			
Skeletal myosin heavy chain	205,000	−10.81	0.984
E. coli β-galactosidase	116,000	−9.55	0.988
Phosphorylase *b*	94,000	−8.66	0.989
Bovine serum albumin	67,000	−7.01	0.988
Hen egg ovalbumin	45,000	−5.29	0.978
S. solfataricus β-glycosidase	109,400[b]	−8.74	0.991
Native PAGE			
Bovine thyroglobulin	660,000	−18.32	0.998
Horse spleen apoferritin	481,000	−12.14	0.998
Sweet potato β-amylase	224,000	−6.84	0.999
Alkaline phosphatase	140,000	−5.84	0.976
S. solfataricus β-glycosidase	233,800[b]	−7.73	0.998

[a] Correlation coefficients *r* for the least square regression analysis used to calculate K_r values.
[b] Values calculated on the basis of the measured K_r of Sβgly, by least square regression analysis of the relationship between log M and log K_r of the marker proteins.

respective values of M (Fig. 3, *panel B*), and the M of Sβgly was then interpolated from the mean square regression linking them. The Ferguson analysis indicated a relative molecular mass of 233,800 for Sβgly in the absence of SDS, a value in good agreement with the calculated M_r (226,760) of the Sβgly tetramer. The values of the apparent relative free mobilities (Y_0) of the reference proteins and Sβgly were ordered in parallel with their relative molecular masses, a circumstance often occurring in practice, because, if the surface charge density remains relatively constant, the larger molecules usually have a higher net charge and free mobility.

In-gel Assay of the Enzymatic Activity of Sβgly with X-Gal—Fig. 4 shows the results of the in-gel chromogenic reaction for 16 h of increasing amounts of Sβgly with 5-bromo-4-chloro-3-indolyl-β-D-galactopyranoside, after electrophoresis in 5% T polyacrylamide gels in 0.05 M sodium phosphate, pH 6.5, both in the presence of 0.1% SDS and in its absence, under which conditions we have documented that the enzyme is in dimeric and tetrameric form, respectively. It appears that the enzymatic activity of Sβgly, as judged from the minimal amount of enzyme giving rise to an appreciable chromogenic reaction, was slightly higher in the presence of SDS (compare the lanes containing 0.10 μg of Sβgly). The lower intensity of the activity staining at the highest doses of Sβgly in the SDS-containing gel was possibly due to an effect of the detergent on the spectral properties of the chromogenic substrate. These results unequivocally proved that the dimeric form of Sβgly was fully active.

Kinetic Analysis and Characterization of the Thermal Stability of Sβgly in the Presence and Absence of SDS—The kinetic analysis of Sβgly indicated an increased activity (k_{cat}) for the enzyme in the presence of SDS, in the temperature range from 30 to 80 °C, and an analogous increase in substrate affinity (K_M) (Table II). In agreement with these results, the Arrhenius

plots of log k_{cat} values against the inverse of the temperature in Kelvin degrees showed a slight decrease in the slope for the enzyme in the presence of SDS (Fig. 5, *panel A*). The activation energies, calculated from the Arrhenius plots, showed values of 75.07 and 78.44 kJ K^{-1} mol^{-1} for the enzyme in the presence and in the absence of SDS, respectively, suggesting a conformational effect of the interaction of Sβgly with SDS on the catalytic site, promoting the reaction. However, these differences decreased as the temperature increased, the ratio of the enzyme activity (V_{max}) in the absence of SDS over that in the presence of SDS (V/V_{SDS}) approaching 1 at 80 °C (Fig. 5, *inset* of *panel A*).

Panel B of Fig. 5 shows the residual activity of Sβgly (expressed as percent of the activity of the native enzyme), measured under standard assay conditions, after 1 h of incubation in the presence and in the absence of SDS, at temperatures ranging from 30 to 80 °C. It appears that after 1 h at 30 °C, Sβgly was more active in the presence of SDS than in its absence. The activities at 40 °C were about 100% in both cases, whereas they fell from 91 to 62% in the presence of SDS, and from 95 to 73% in its absence, in the interval 50–80 °C (Fig. 5, *panel B*). These data indicated a reduced thermostability of Sβgly in the presence of SDS.

Solvent-accessible Surfaces of Various Oligomerization States of Sβgly, Charge Distribution, and Molecular Contacts of Intersubunit Contact Surfaces in A-C and A-D Dimers—The availability of a crystal structure for Sβgly (10) prompted us to a detailed and direct analysis of the protein interfaces involved in the dissociation of Sβgly into dimers. The crystal state, however, represents a limiting case of reduced mobility/low entropy, which, in principle, cannot be directly correlated with

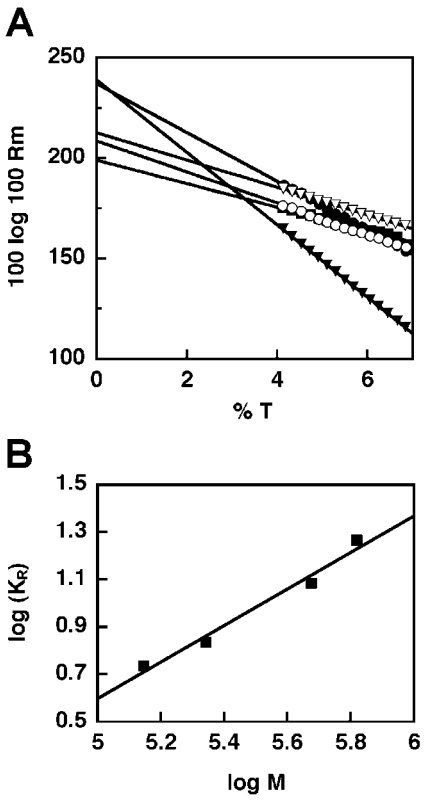

FIG. 3. **Ferguson analysis of the PAGE in native conditions of *S. solfataricus* β-glycosidase.** *Panel A* shows the Ferguson plot constructed for the set of reference proteins and Sβgly. Each protein was subjected to electrophoresis on two replicate 4–7% T, 2.7% C polyacrylamide transverse-gradient gels. Electrophoresis was performed in Tris/boric acid without SDS, according to Neville (16). Symbols are as follows: *filled triangle*, bovine thyroglobulin; *filled circle*, horse spleen apoferritin; *open triangle*, sweet potato β-amylase; *filled square,* alkaline phosphatase; *open circle*, Sβgly. For the sake of clarity, only a single set of points from one gel per each couple is shown. The values of K_r obtained are reported in Table I. *Panel B* shows the plot of the log of measured K_r *versus* log M of the reference proteins used to interpolate the log M of Sβgly.

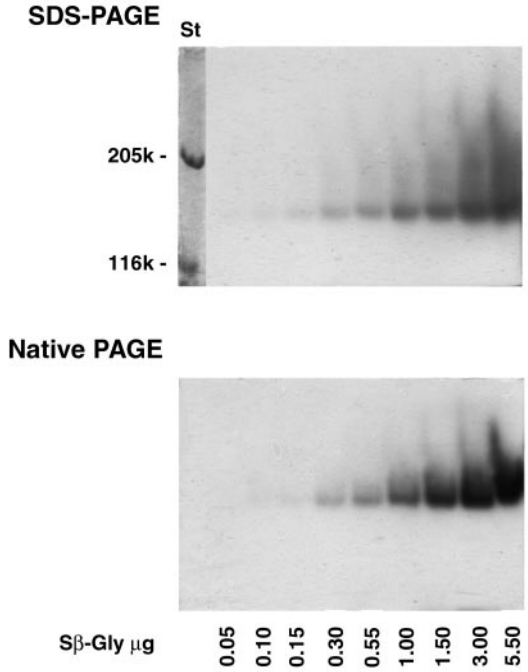

FIG. 4. **In-gel assay of the enzymatic activity of *S. solfataricus* β-glycosidase with X-gal after PAGE both in SDS and in native conditions.** Electrophoresis was conducted in 5% total acrylamide gels containing 0.375 M Tris/HCl, pH 8.6, with (*upper panel*) or without 0.1% SDS (*lower panel*). After electrophoresis, the gels were equilibrated in 0.05 M sodium phosphate, pH 6.5, with or without 0.1% SDS, and then incubated in 10% (w/v) X-gal in 0.05 M sodium phosphate, pH 6.5, 10% (v/v) methanol, with or without 0.1% SDS, for 16 h at 37 °C. In the *upper gel*, the *leftmost lane*, containing the relative molecular mass standards (*St*), was cut off and separately stained with Coomassie Brilliant Blue R-250. The amounts of Sβgly in each lane are indicated at the *bottom* of the gels.

TABLE II

Kinetic constants at several temperatures (from 30 to 80 °C) of S. solfataricus β-glycosidase in the presence and absence of SDS, using PNPG as the substrate

Temperature	*S. solfataricus* β-glycosidase			*S. solfataricus* β-glycosidase in SDS		
	K_M	k_{cat}	k_{cat}/K_M	K_M	k_{cat}	k_{cat}/K_M
°C	mM	s^{-1}	mM^{-1} s^{-1}	mM	s^{-1}	mM^{-1} s^{-1}
30	0.5	12.6	25.2	0.2	18.3	91.3
40	0.5	33.0	65.9	0.2	45.6	228.0
50	0.5	85.7	171.4	0.2	115.4	577.0
60	0.5	212.1	424.2	0.2	257.2	1285.8
70	0.5	474.7	949.4	0.2	534.1	2670.4
80	0.5	997.8	1995.6	0.2	1059.3	5296.6

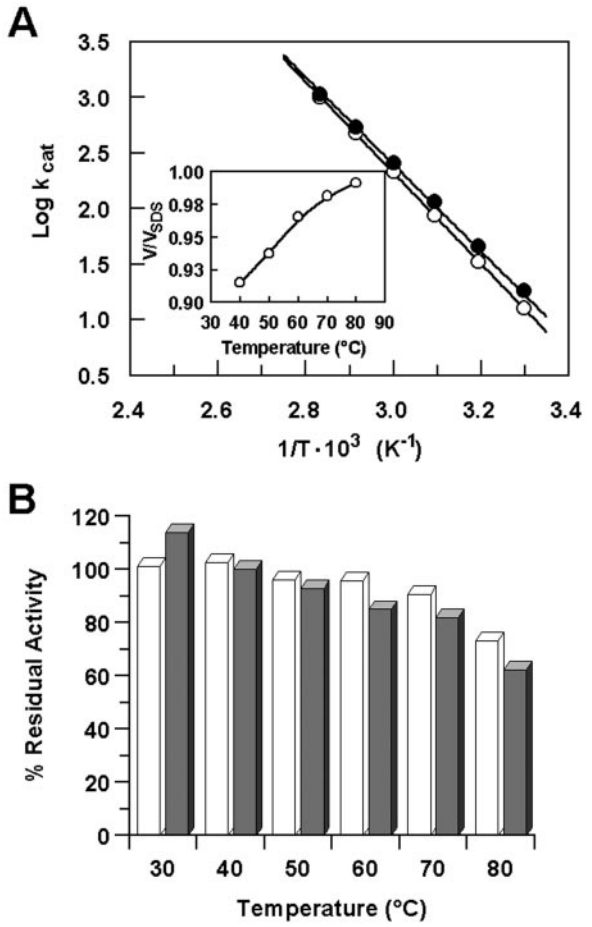

FIG. 5. *Panel A*, Arrhenius plot of the logarithm of activity (k_{cat}) against the inverse of temperature in K degrees of the enzyme in the presence (*filled circle*) and absence (*open circle*) of SDS. *Inset* in *panel A*, ratio between the enzyme activities at various temperatures in the absence (V) and in the presence of SDS (V_{SDS}). *Panel B*, residual activity of Sβgly after 1 h of incubation in the absence (*open bars*) and presence (*filled bars*) of SDS at several temperatures, in the range 30–80 °C, expressed as percent of the activity of the native enzyme, measured under standard assay conditions (see "Experimental Procedures").

the observed behavior of inter-subunit interfaces at standard, as well as at high temperature, and/or in the presence of SDS. In this view, we used a combination of computational simulation tools and approaches, which could provide a more reliable description of both the static and the dynamic features responsible for the observed aggregation state and functional properties. The methods ranged from a mere analysis of the PDB 1GOW entry, and simple energy minimization (EM) calculations, performed in order to fix the position of hydrogen atoms and include those first-shell solvation water molecules, which were missing in the PDB entry, to molecular dynamics (MD) simulations performed at different temperatures (300, 310, and 368 K). As the increase in simulated temperature led, as a macroscopic result, to a progressive desolvation of the intermonomeric interfaces, the limiting cases of totally desolvated Sβgly tetramers, A-C and A-D dimers were also simulated by EM and MD approaches. The most striking result in the comparative analysis of all the computational results was the substantial conservation of the general features of the interfaces (especially for the A-C interface). In fact, as the degree of solvation decreased in MD simulations in water solution, only local rearrangements of the interaction patterns were observed, with the progressive substitution of water-mediated polar interactions with direct intermonomeric H-bonds or salt bridges. The relative weight of the latter interactions increased

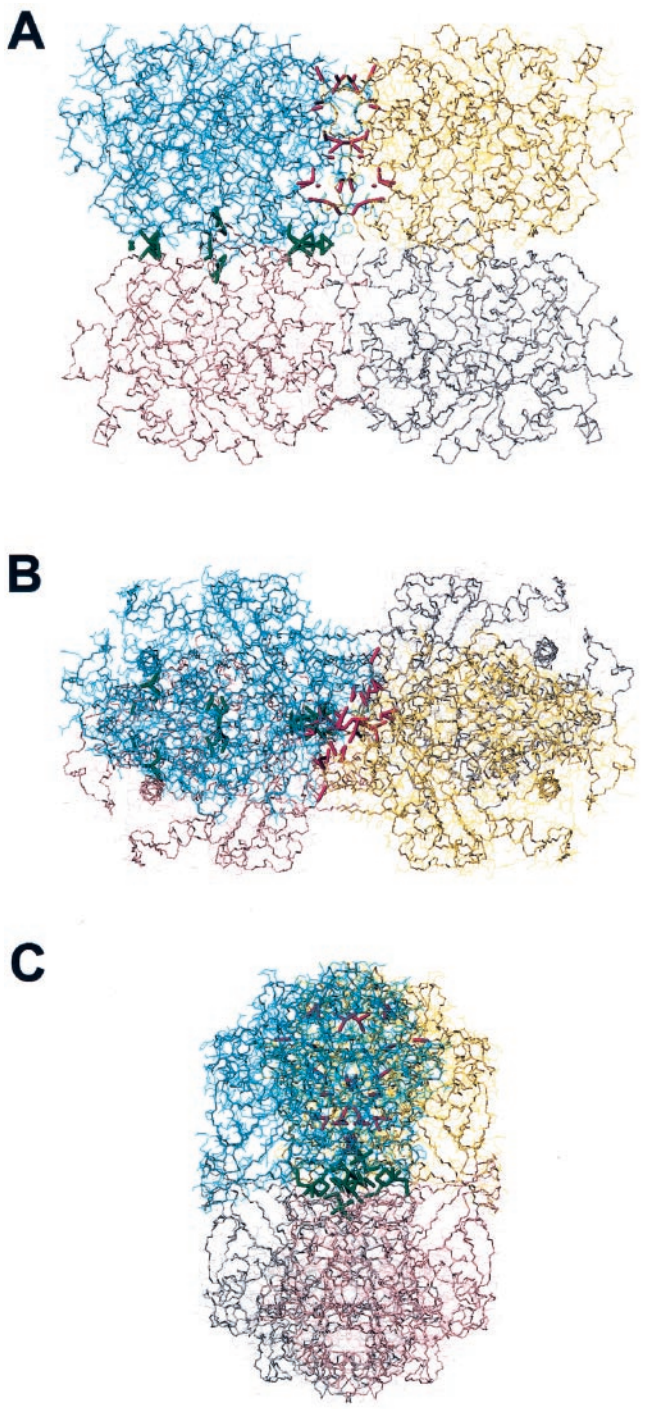

FIG. 6. **Wire representation of the SβGly tetramer.** Color codes for subunits are as follows: A chain, *cyan*; B chain, *gray*; C chain, *yellow*; D chain, *pink*. Amino acid residues involved in H-bonds and salt bridges between monomers are shown in *stick* format and are *magenta* for the A-C interface and *green* for the A-D interface. *Panels B* and *C* were obtained by rotating the structure shown in *panel A* by 90° around the horizontal and vertical axes, respectively.

as the interface solvation decreased (high temperature and/or lack of explicit solvent). In this view, although most of the following analysis was performed on the experimental crystal structure or on the fully desolvated system, the described features were substantially insensitive to simulation conditions, unless explicitly stated.

An analysis of the solvent-accessible surface (SAS) of the Sβgly tetramer, the two possible dimers (A-C and A-D in Fig. 6), and the monomer in the Sβgly tetramer crystal structure

TABLE III
Solvent-accessible surface areas of different oligomerization states of S. solfataricus β-glycosidase

System	Solvent-accessible surface (Å^2)				Charged/total
	Positively charged	Negatively charged	Polar	Total	
					%
Monomer	2433	1931	8053	18253	24
A-C dimer	4570	3653	15248	34026	24
A-D dimer	4533	3737	15428	34772	24
Tetramer	8385	7057	29066	64363	24

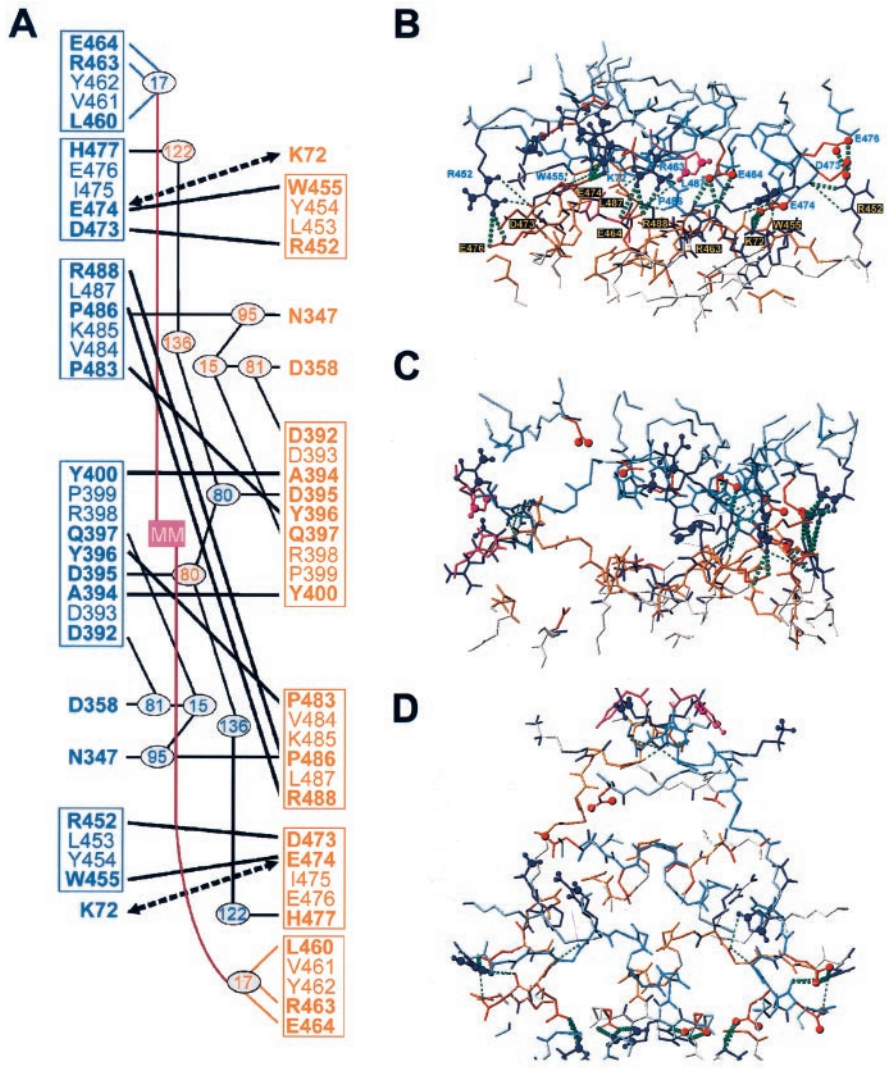

FIG. 7. *Panel A*, schematic representation of the polar interaction network at the intermonomeric interface of the SβGly A-C dimer, as it results from the analysis of the SβGly crystal structure, after simple EM calculations. Amino acid residues and water molecules pertaining to monomers A and C are depicted in *cyan* and *orange*, respectively. Contiguous residues are *boxed*, and those involved in interactions are in *boldface type*. Salt bridges are represented by *dashed lines* with *arrowheads*, H-bonds by *thick lines*, and water-mediated interactions by *thin lines*. Water molecules are indicated by *gray ovals* marked by the *numbers* that identify them in the PDB file. A water molecule (*MM*) introduced in an "empty" spot between the two H_2O molecules number 17, and its interactions are depicted in *violet*. *Panels B–D*, *stick* representation of the polar interaction network at the intermonomeric interface of the desolvated SβGly A-C dimer as it results form the MD simulation performed at 368 K. For clarity, only the backbone is drawn, except for polar residues making contacts at the interface, whose heavy side chain and polar hydrogen atoms are also plotted. Residues making interchain contacts within 6 Å and their numbers are colored in *cyan* and *orange* for A and C monomers, respectively, whereas the other interface residues are represented in *light blue* and *yellow*. For the sake of clarity, only some residues per monomer are indicated. Acidic and basic side chains of A and C monomers are shown in *red* and *blue*, respectively, except for the C-terminal His, which is drawn in *magenta*, whereas a *ball* representation is used for polar atoms of these residues in the A chain. *Thin dotted green sticks* represent H-bonds, and *thicker sticks* represent salt bridges. The views in *panels C* and *D* were obtained by rotating the structure 90° around the vertical and horizontal axes, respectively.

showed that the changes in exposed area, going from the tetramer to the two possible dimers, were different. In particular, A-D exhibited a larger exposed surface (34,771.8 *versus* 34,026.5 Å^2 in A-C), with larger components both in the polar (15,428.3 *versus* 15,248.0 Å^2 in A-C) and in the hydrophobic surfaces (Table III). Polar interaction analysis showed that the A-C dimer, exhibiting the lowest SAS area, was also more stabilized by a network of salt bridges either mediated by the solvent, as observed in the energy-minimized dimer, as refined from the crystal structure of the tetramer (Fig. 6; Fig. 7, *panel A*; Table IV), or direct, as detected in MD simulations of the dimer without explicit solvation (Fig. 7, *panel B*). It is interesting to note that the intermolecular framework of polar interactions was substantially preserved, despite the extensive rearrangement involving the contact surface of the polar residues. Another interesting feature of the A-C interface was the microscopic charge distribution in the region surrounding the polar interaction network. In fact, the electrostatic field calculated for the A-C dimer in that region exhibited a local short range anisotropy, despite the substantial global neutrality associated with the presence of ionic couples. This was because of an average higher preference of the negatively charged residues for the dimer surface, compared with the positions of the corresponding positively charged residues, on the average more embedded in the A-C interface (Fig. 8, *panel A*). This feature could be related both to the unusually high resistance to dissociation of this dimer in SDS, due to the unfavorable interactions of the negatively charged SDS polar groups with the interface region, and to the anomalous migration observed in SDS-PAGE, due to the relatively low affinity of a large exposed interface region for SDS binding.

A comparison between the protein monomeric structures,

TABLE IV

H-bonds (including H_2O) in the network at the interface of the A-C dimer from the PDB file (1GOW) of the Sβgly tetramer

The abbreviations used are: HA, H_2O crystallographically associated with the A chain; HC, H_2O associated by crystallographic symmetry with the C chain; SB, salt bridge.

Chain	Residue	Heavy atom	Chain	Residue	Heavy atom	Distance
						Å
A	72Lys$^+$	NZ	C	474Glu$^-$	OE1	3.32 SB
A	72Lys$^+$	NZ	C	474Glu$^-$	OE2	3.16 SB
A	347Asn	ND2	HA	95H_2O	O	3.36
A	358Asp$^-$	OD1	HA	81H_2O	O	2.79
A	358Asp$^-$	OD2	HA	81H_2O	O	3.17
A	392Asp$^-$	OD1	HA	81H_2O	O	2.87
A	394Ala	O	C	400Tyr	OH	2.71
A	395Asp$^-$	OD2	HC	80H_2O	O	3.25
A	395Asp$^-$	O	HC	80H_2O	O	3.30
A	396Tyr	OH	C	483Pro	O	2.93
A	397Gln	NE2	HA	15H_2O	O	3.05
A	400Tyr	OH	C	394Ala	O	2.71
A	452Arg$^+$	NH2	C	473Asp$^-$	O	3.22
A	455Trp	N	C	474Glu$^-$	O	2.76
A	460Leu	O	A	17H_2O	O	2.81
A	463Arg$^+$	NH1	A	17H_2O	O	2.62
A	464Glu$^-$	OE2	A	17H_2O	O	2.70
A	473Asp$^-$	O	C	452Arg$^+$	NH2	3.22
A	474Glu$^-$	OE1	C	72Lys$^+$	NZ	3.32 SB
A	474Glu$^-$	OE2	C	72Lys$^+$	NZ	3.16 SB
A	474Glu$^-$	O	C	455Trp	N	2.76
A	477His$^+$	NE2	HC	122H_2O	O	3.28
A	483Pro	O	C	396Tyr	OH	2.93
A	486Pro	O	C	488Arg$^+$	N	2.90
A	486Pro	O	HC	95H_2O	O	2.84
A	488Arg$^+$	N	C	486Pro	O	2.90
HA	80H_2O	O	C	395Asp$^-$	OD2	3.25
HA	80H_2O	O	C	395Asp$^-$	O	3.30
HA	80H_2O	O	HC	80H_2O	O	2.60
HA	95H_2O	O	C	486Pro	O	2.84
HA	122H_2O	O	C	477His$^+$	NE2	3.28
C	347Asn	ND2	HC	95H_2O	O	3.36
C	358Asp$^-$	OD1	HC	81H_2O	O	2.79
C	358Asp$^-$	OD2	HC	81H_2O	O	3.17
C	392Asp$^-$	OD1	HC	81H_2O	O	2.87
C	397Gln	NE2	HC	15H_2O	O	3.05
C	460Leu	O	HC	17H_2O	O	2.80
C	463Arg$^+$	NH1	HC	17H_2O	O	2.62
C	464Glu$^-$	OE2	HC	17H_2O	O	2.70

going from the native tetramer to the calculated A-C dimer, showed that the only relevant rearrangement occurring in the interface region involved the C-terminal His residues. In the tetramer these residues were swapped among the different monomers, the C-terminal His in chain A mainly interacting with the B and D chains, whereas in the A-C dimer new direct salt bridge and H-bond interactions were formed. These interactions were fully integrated in the intermolecular salt bridge framework, ensuring the closure of the network and the shielding of the hydrophobic core of the interface from the solvent.

Another important structural feature observed in the comparison between the Sβgly tetramer and the two possible dimers involved the accessibility of the Sβgly active site which, in the case of the A-C dimer, was substantially increased, in comparison with both the tetramer and the A-D dimer (Fig. 8, *panel B*). This increased accessibility resulted from the loss of a "wall" partially surrounding the mouth of the active site cavity. In the case of the A monomer, the wall was contributed by the D monomer, whose loss in the A-C dimer could thus be responsible for the increased activity of dimeric Sβgly in SDS, by determining a facilitated diffusion of the substrates and/or the final products.

DISCUSSION

This study documents that homotetrameric β-glycosidase from *S. solfataricus* dissociates incompletely in SDS into dimers, whose apparent relative molecular mass, measured by Ferguson analysis of polyacrylamide transverse gradient gels in SDS, was 109,400 (Table I). Thus, the apparent relative molecular mass of 160,000 of Sβgly in SDS-PAGE (Fig. 1) was the result of anomalous migration.

The estimation of the relative molecular mass of proteins in SDS-PAGE by the commonly used plot of $-\log R_m$ *versus* M (28) resides on the assumptions that the electrophoretic mobility of polypeptide chains in SDS is a unique function of their relative molecular mass, and the apparent relative free mobility Y_0 (*i.e.* the apparent relative mobility at 0 acrylamide concentration) is the same for all the standard and unknown protein-SDS complexes (16). Although the values of Y_0 of many protein-SDS complexes are nearly constant, deviations are known, which may be due to untypical binding of SDS, significant contribution of the intrinsic protein charge to the net charge of the protein-SDS complex, or substantial deviation from the usual symmetry of protein-SDS complexes (16).

Ferguson plots of the logarithm of the relative mobility (R_m) of a protein at several different acrylamide concentrations against the gel concentration (T) (29) was shown to describe adequately the behavior of 17 globular proteins, varying in relative mass from 45,000 to 500,000 (27). Neville (16) validated the use of the Ferguson analysis for PAGE in SDS. For a number of multimeric proteins with relative molecular mass values between 60,000 and 900,000, M values estimated by the use of plots of log K_r *versus* log M differed from the actual

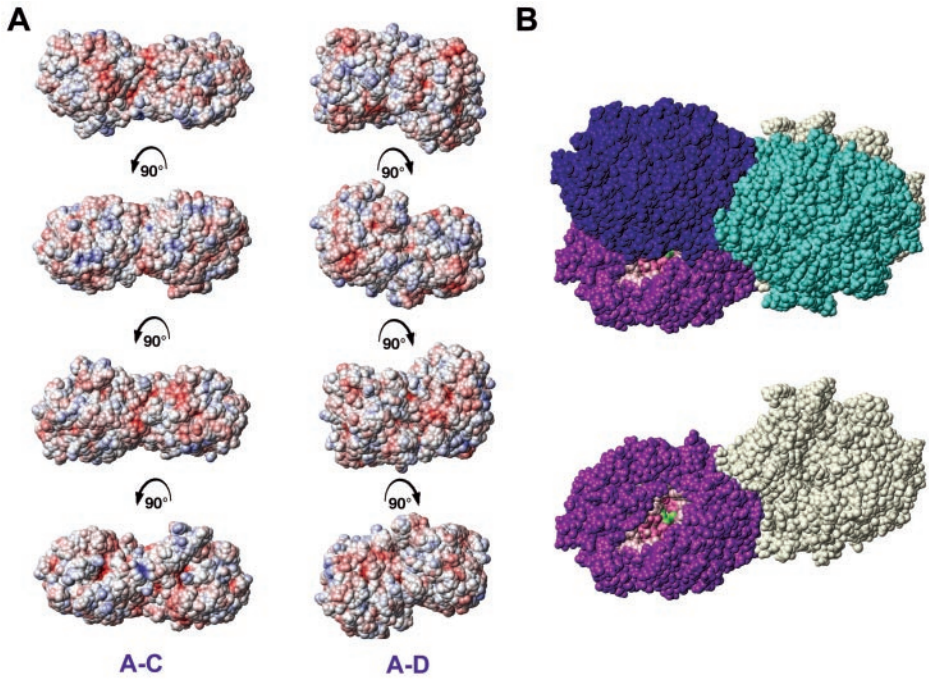

FIG. 8. *Panel A*, molecular electrostatic potential in A-C and A-D SβGly dimers. A molecular electrostatic potential projection on the solvent-accessible surface is shown, with negative and positive potential regions shown in increasingly darker shades of *red* and *blue*, respectively. The four views of each dimer correspond to subsequent rotations of 90° around the horizontal axis of the plot. *Panel B*, accessibility of the active site of SβGly in the tetramer *versus* the A-C dimer. Van der Waals sphere representation of the SβGly tetramer and A-C dimer, where A, B, C, and D SβGly chains are shown in *violet*, *cyan*, *light yellow*, and *blue*, respectively. For the monomer, the three active site residues (His-150, Glu-206, and Glu-387) are shown in *green*, and residues within 6 and 12 Å from the active site are shown in *deep* and *light pink*, respectively.

values by no more than 10%, the average error being 5% (30). Van Lith *et al.* (31) demonstrated the accuracy of Ferguson plots constructed with transverse-gradient polyacrylamide gels.

The Ferguson analysis was indicated in our case for the following reasons. 1) Because K_r is a measure of the effective molecular surface area (or the radius of a sphere with the same surface area) (32, 33), and also the K_r of protein-SDS complexes is a unique function of their polypeptide chain length. Thus, plots of log K_r *versus* log M are linear and can be used to read off the value of log M from the K_r value, even of proteins or SDS-protein complexes having extended or non-typical shapes. 2) Unlike gel filtration and sedimentation, Ferguson plots of polyacrylamide gels did not sense the presence of SDS and thus permitted us to determine accurately the mass of the pure protein and the oligomerization state of Sβgly, both in the presence and in the absence of the detergent. The relative molecular masses determined for Sβgly in the presence of SDS (109,400) and in its absence (233,800) (Table I) differed from mass spectrometric and calculated masses (113,380 and 226,760, respectively) by −3.5% and +3.1%, respectively.

We analyzed the possible determinants of the resistance of dimeric Sβgly to the dissociation by SDS. An analysis of the solvent-accessible surfaces, based on the crystal structure of the enzyme resolved at 2.6 Å (10), showed that the change in exposed surface area was higher, going from the tetramer to the A-C dimer in comparison with the A-D dimer (Table III). EM calculations, MD simulations, and polar interaction analysis showed that the A-C intermonomeric interface was more stabilized by a network of polar interactions, either direct or solvent-mediated (Table IV and Figs. 6 and 7), which was surrounded by a relatively large area characterized by an average higher preference of the negatively charged residues for the A-C dimer surface. Other negatively charged surface patches were also detected, the largest one surrounding the active site of Sβgly (Fig. 8, *panel A*). The resulting unfavorable interaction of the negatively charged polar groups of SDS with these regions may have contributed both to the unusually high resistance to dissociation of the A-C dimer in SDS and to the binding of an untypical amount of SDS, thus preventing the shape changes usually observed after the binding of SDS to proteins and resulting in a highly asymmetric shape of the SDS-Sβgly A-C dimer complex. In fact, the hydrodynamic properties of the latter appeared to be significantly different from those of standard protein-SDS complexes, as judged by its anomalous migration (Fig. 1) and its lower than normal free mobility (Y_0) in SDS-PAGE (Fig. 2). A highly asymmetric shape of the SDS-calsequestrin complex was invoked to explain the anomalously slow migration of calsequestrin in SDS-PAGE at alkaline pH (34). The dominant role of the unfavorable interaction of the A-C interface of Sβgly with SDS in determining these effects is underscored by the normalization of the apparent mass of the Sβgly monomers in SDS-PAGE, after dissociation of Sβgly in organic solvents (Fig. 1).

The observation that Sβgly is dimeric, in the presence of 0.1–1.0% SDS, is consistent with our previous report (13) that 0.1% SDS had little effect on the secondary structure of Sβgly, as monitored by far-UV and IR spectroscopy. In this view, the changes observed in near-UV CD spectra (12, 13) could be mainly attributed to changes in quaternary structure.

Previous studies (12) had also reported an increase of the enzymatic activity of Sβgly at 30 °C, in the presence of 0.05–0.1% SDS. The present data provide a mechanistic basis for this effect by showing that Sβgly activation in SDS coincides with its dissociation into dimers. In fact, the kinetic analysis of the enzyme in the presence of 0.1% SDS, at several temperatures, indicated a slightly lower E_a value (Fig. 5, *panel A*) and corresponding increases in activity (k_{cat}) and affinity (K_M) for the synthetic substrate PNPG (Table II). These observations could be explained by a facilitated access of the substrate to the active site of the enzyme, upon dissociation into dimers. In fact, EM and MD simulation analyses of the crystal structure of

Sβgly showed an increased accessibility of the catalytic site and a diminished steric hindrance for the substrate in the catalytic tunnel, after dissociation of the tetramer into the A-C and B-D dimers, (Fig. 8, *panel B*). An SDS-conformational change facilitating the access of the substrate to the dicopper active site was invoked to explain also the strong specific activation of tyrosinase from *Marinomonas mediterranea* by submicellar concentrations of SDS (35). Other examples of SDS-induced conformational changes activating enzymatic functions include the SDS-induced *O*-diphenoloxidase activity of hemocyanins of some chelicerates and crustaceans. In these cases, it was suggested that SDS may mimic the function of hydrophobic and/or polar effectors, by inducing conformational conversion without denaturation (36).

Considering that Sβgly does not exhibit allosteric behavior (8), the availability of a tetrameric and a dimeric form of the enzyme, both endowed with enzymatic activity, makes Sβgly a potentially useful model for the study of the relationships between oligomerization and physicochemical properties other than catalytic activity and allosteric regulation. This is also from an evolutionary point of view.

Two recent examples of protein resistance to dissociation by SDS deserve the closest attention, because of their biological implications.

One such case concerns the heterodimeric proteins responsible in humans for the presentation of foreign and self-antigens to the cells of the immune system, encoded by the major histocompatibility complex class II genes of the HLA complex. Genetic associations between different alleles at these polymorphic loci, particularly some HLA-DQ alleles, and susceptibility or protection with respect to important human autoimmune diseases, such as insulin-dependent diabetes mellitus, have been detected in population and case-control studies (37). Studies on HLA-DQ αβ dimers have revealed a correlation between SDS stability, binding of antigenic peptides, and IDDM susceptibility, such that the most SDS-stable molecules were encoded by IDDM susceptibility alleles (1). Similar observations were made for the mouse I-A αβ dimers, such that the I-A molecule in genetically susceptible non-obese diabetic mice was least SDS-stable, compared with other I-A molecules (38). Mutagenesis studies of the polymorphic residues essential for the SDS stability of the HLA dimer DQ0602 indicated the critical role of Asp at position β57 and the modulating role of residues at positions β30, β70, and β86 (4), whereas a modeled structure, constructed by homology on the crystal structure of the related molecule HLA-DR1, located these residues within the antigenic peptide-binding groove of the molecule and showed Asp-β57 engaged in the formation of a salt bridge with Arg-α79 (5).

Another case concerns apoE, a component of several classes of lipoproteins and a major non-amyloid component of the extracellular senile plaques of Alzheimer's disease, in which it is stably complexed with amyloid-β (Aβ). ApoE interacts in an isoform-specific manner with Aβ to form an SDS-stable complex. Native apoE2 and apoE3 form SDS-stable complexes with Aβ with much greater avidity than apoE4 (2), which is present with increased frequency in patients with sporadic and late-onset familial AD, and is considered a risk factor for the disease (3). Nearly all Aβ in plaque-free, non-AD brains is bound in SDS-stable complexes with apoE, in which it is more susceptible to proteases. Thus, the interaction with apoE seems to favor the sequestration and degradation of neurotoxic species of Aβ in the human brain (39). Competition and mutagenesis studies aimed at identifying the basis for the SDS-stable apoE3-Aβ complex formation indicated the critical role of residues 13–28 of Aβ, interacting with residues at the C terminus of Aβ (6), and of a salt bridge between Arg-61 and Asp-65 of apoE3 (7).

Ionic interactions were identified, in the examples cited, among the determinants of the stability of supramolecular assemblies to the dissociation by SDS. However, their description was limited to a single salt bridge, a certain degree of incompleteness being inherent in the methods adopted, such as point mutagenesis and molecular modeling. On the other hand, by refining the crystal structure of Sβgly by the means of EM calculations and MD simulations, we attained a systematic description of the intermolecular contacts involved in the stabilization of the A-C dimer, in which multiple polar interactions appeared to exert a dominating role as part of a highly organized network (Fig. 6 and Fig. 7 and Table IV). The extended network of H-bonds and ionic interactions in the intermonomeric A-C interface of Sβgly, in addition to stabilizing the A-C dimer against dissociation by SDS, seemed to be also involved in determining its thermal stability. In fact, the measurements of the enzyme stability at several temperatures indicated that the Sβgly dimer, in the presence of SDS, retained at least 85% of the stability of the native tetramer to the temperature perturbation (Fig. 5, *panel B*). The role of ionic interactions, and especially their networks, in determining the increased thermal stability of several thermophilic proteins has been well documented (40–46). Complex ionic interactions (47) were especially capable of enhancing stability through a cooperative strengthening mechanism (48). Theoretical models (49) show that salt bridges are preferentially stabilized at high temperatures, because the desolvation penalty in the association of two charged residues to form a salt bridge is markedly reduced. In accordance with these facts, the structural analysis of the A-C interface showed a peculiar resilience of the polar interaction network. Its rearrangement capabilities preserved substantial interactions under a wide range of conditions of solvation and relative entropic *versus* enthalpic stabilization (crystal state, solution state at room or high temperature, and total lack of water molecules) (Table IV and Fig. 7), supporting its stabilizing role under both normal and extreme conditions.

In conclusion, we present a detailed investigation of the mechanistic basis of the observed resistance of dimeric Sβgly to dissociation by SDS. The description of the network of polar interactions stabilizing the A-C intermonomeric interface, as it results from the analysis of the crystal structure of Sβgly and its refinement by EM analysis and MD simulations under various solvation conditions, may be useful for our understanding of the properties of other SDS-resistant protein complexes of medical importance and for protein engineering purposes.

Acknowledgment—We thank Prof. Mosè Rossi for critical reading of the manuscript and support.

REFERENCES

1. Ettinger, R. A., Liu, A. W., Nepom, G. T., and Kwok, W. W. (1998) *J. Immunol.* **161,** 6439–6445
2. LaDu, M. J., Pederson, T. M., Frail, D. E., Reardon, C. A., Getz, G. S., and Falduto, M. T. (1995) *J. Biol. Chem.* **270,** 9030–9042
3. Corder, E. H., Saunder, S. M., Strittmatter, W. J., Schmechel, D. E., Gaskell, P. C., Small, G. W., Roses, A. D., Haines, J. L., and Pericak-Vance, M. A. (1993) *Science* **261,** 921–923
4. Ettinger, R. A., Liu, A. W., Nepom, G. T., and Kwok, W. W. (2000) *J. Immunol.* **165,** 3232–3238
5. Sanjeevi, C. B., DeWeese, C., Landin-Olsson, M., Kockum, I., Dahlquist, G., and Lenmark, A. (1997) *Tissue Antigens* **50,** 61–65
6. Munson, G. W., Roher, A. E., Kuo, Y.-M., Gilligan, S. M., Reardon, C. A., Getz, G. S., and LaDu, M. J. (2000) *Biochemistry* **39,** 16119–16124
7. Bentley, N. M., LaDu, M. J., Rajan, C., Getz, G. S., and Reardon, C. A. (2002) *Biochem. J.* **366,** 273–279
8. Nucci, R., Moracci, M., Vaccaro, C., Vespa, N., and Rossi, M. (1993) *Biotechnol. Appl. Biochem.* **17,** 239–250
9. Schiffmann, R., and Brady, R. O. (2002) *Drugs* **62,** 733–742
10. Aguilar, C. F., Sanderson, I., Moracci, M., Ciaramella, M., Nucci, R., Rossi, M., and Pearl, L. H. (1997) *J. Mol. Biol.* **271,** 789–802
11. Henrissat, B. (1998) *Biochem. Soc. Trans.* **26,** 153–156
12. Nucci, R., D'Auria, S., Febbraio, F., Vaccaro, C., Morana, A., De Rosa, M., and Rossi, M. (1995) *Biotechnol. Appl. Biochem.* **21,** 265–274
13. D'Auria, S., Barone, R., Rossi, M., Nucci, R., Barone, G., Fessas, D., Bertoli, E., and Tanfani, F. (1997) *Biochem. J.* **323,** 833–840

14. Laemmli, U. K. (1970) *Nature* **227,** 680–685
15. Gentile, F., Veneziani, B. M., and Sellitto, C. (1997) *Anal. Biochem.* **244,** 228–232
16. Neville, D. M. (1971) *J. Biol. Chem.* **246,** 6328–6334
17. de Haën, C. (1987) *Anal. Biochem.* **166,** 235–245
18. Weiner, P. K., and Kollman, P. A. (1981) *J. Comput. Chem.* **2,** 287–303
19. Weiner, S. J., Kollman, P. A., Case, D. A., Chandra Singh, U., Ghio, C., Alagona, G., Profeta, S., and Weiner, P. K. (1984) *J. Am. Chem. Soc.* **106,** 765–784
20. Weiner, S. J., Kollman, P. A., Nguyen, D. T., and Case, D. A. (1986) *J. Comput. Chem.* **7,** 230–252
21. Cornell, W. D., Cieplak, P., Bayly, C. I., Gould, I. R., Merz, K. M., Jr., Ferguson, D. M., Spellmeyer, D. C., Fox, T., Caldwell, J. W., and Kollman, P. A. (1995) *J. Am. Chem. Soc.* **117,** 5179–5197
22. Ryckaert, J. P., Ciccotti, G., and Berendsen, H. J. C. (1977) *J. Comp. Phys.* **23,** 327–341
23. Berendsen, H. J. C., Postma, J. P. M., van Gunsteren, W. F., Di Nola, A., and Haak, J. M. (1984) *J. Chem. Phys.* **81,** 3684–3690
24. Koradi, R., Billeter, M., and Wüthrich, K. (1996) *J. Mol. Graphics* **14,** 51–55
25. McDonald, I. K., and Thornton, J. M. (1994) *J. Mol. Biol.* **238,** 777–793
26. Wessel, D., and Flügge, U. I. (1984) *Anal. Biochem.* **138,** 141–143
27. Hedrick, J. L., and Smith, A. J. (1968) *Arch. Biochem. Biophys.* **126,** 155–164
28. Weber, K., and Osborn, M. (1969) *J. Biol. Chem.* **244,** 4406–4412
29. Ferguson, K. A. (1964) *Metab. Clin. Exp.* **13,** 985–1002
30. Bryan, J. K. (1977) *Anal. Biochem.* **78,** 513–519
31. Van Lith, H. A., Haller, M., Van Zutphen, L. F. M., and Beynen, A. C. (1992) *Anal. Biochem.* **201,** 288–300
32. Rodbard, D., and Chrambach, A. (1970) *Proc. Natl. Acad. Sci. U. S. A.* **65,** 970–977
33. Rodbard, D., and Chrambach, A. (1971) *Anal. Biochem.* **40,** 95–134
34. Cozens, B., and Reithmeier, R. A. F. (1984) *J. Biol. Chem.* **259,** 6248–6252
35. Lopez-Serrano, D., Sanchez-Amat, A., and Solano, F. (2002) *Pigm. Cell Res.* **15,** 104–111
36. Decker, H., Ryan, M., Jaenicke, E., and Terwilliger, N. (2001) *J. Biol. Chem.* **276,** 17796–17799
37. Sanjeevi, C. B., Landin-Olsson, M., Kockum, I., Dahlquist, G., and Lenmark, A. (1995) *Tissue Antigens* **45,** 148–152
38. Carrasco-Marin, E., Shimizu, J., Kanagawa, O., and Unanue, E. R. (1996) *J. Immunol.* **156,** 450–458
39. Russo, C., Angelini, G., Dapino, D., Piccini, A., Piombo, G., Schettini, G., Chen, S., Teller, J. K., Zaccheo, D., Gambetti, P., and Tabaton, M. (1998) *Proc. Natl. Acad. Sci. U. S. A.* **95,** 15598–15602
40. Walker, J. E., Wonacott, A. J., and Harris, J. I. (1980) *Eur. J. Biochem.* **108,** 581–586
41. Chan, M. K., Mukund, S., Kletzin, A., Adams, M. W., and Rees, D. C. (1995) *Science* **267,** 1463–1469
42. Korndörfer, I., Steipe, B., Huber, R., Tomschy, A., and Jaenicke, R. (1995) *J. Mol. Biol.* **246,** 511–521
43. Tomschy, A., Böhm, G., and Jaenicke, R. (1994) *Protein Eng.* **7,** 1471–1478
44. Kelly, C. A., Nishiyama, M., Ohnishi, Y., Beppu, T., and Birktoft, J. J. (1993) *Biochemistry* **32,** 3913–3922
45. Spassov, V. Z., Karshikoff, A. D., and Ladenstein, R. (1995) *Protein Sci.* **4,** 1516–1527
46. Vogt, G., Woell, S., and Argos, P. (1997) *J. Mol. Biol.* **269,** 631–643
47. Musafia, B., Buchner, V., and Arad, D. (1995) *J. Mol. Biol.* **254,** 761–770
48. Horovitz, A., Serrano, L., Avron, B., Bycroft, M., and Fersht, A. R. (1990) *J. Mol. Biol.* **216,** 1031–1044
49. Elcock, A. H. (1998) *J. Mol. Biol.* **284,** 489–502

SDS-resistant Active and Thermostable Dimers Are Obtained from the Dissociation of Homotetrameric β-Glycosidase from Hyperthermophilic *Sulfolobus solfataricus* in SDS: STABILIZING ROLE OF THE A-C INTERMONOMERIC INTERFACE

Fabrizio Gentile, Pietro Amodeo, Ferdinando Febbraio, Francesco Picaro, Andrea Motta, Silvestro Formisano and Roberto Nucci

J. Biol. Chem. 2002, 277:44050-44060.
doi: 10.1074/jbc.M206761200 originally published online September 3, 2002